Katanin p80 Regulates Human Cortical Development by Limiting Centriole and Cilia Number

Wen F. Hu,[1,2,3,5,6] Oz Pomp,[19] Tawfeg Ben-Omran,[12] Andrew Kodani,[18] Katrin Henke,[4,9] Ganeshwaran H. Mochida,[1,2,7,10] Timothy W. Yu,[1,7,11] Mollie B. Woodworth,[1,2,3,7] Carine Bonnard,[19] Grace Selva Raj,[19] Thong Teck Tan,[19] Hanan Hamamy,[21] Amira Masri,[23] Mohammad Shboul,[19] Muna Al Saffar,[1,2,13] Jennifer N. Partlow,[1,2,3] Mohammed Al-Dosari,[17] Anas Alazami,[14] Mohammed Alowain,[15,16] Fowzan S. Alkuraya,[14,16] Jeremy F. Reiter,[18] Matthew P. Harris,[4,9,24,*] Bruno Reversade,[19,20,22,24,*] and Christopher A. Walsh[1,2,3,5,6,7,8,24,*]
[1]Division of Genetics and Genomics, Department of Medicine
[2]Manton Center for Orphan Disease Research
[3]Howard Hughes Medical Institute
[4]Department of Orthopedic Research
Boston Children's Hospital, Boston, MA 02115, USA
[5]Program in Neuroscience
[6]Harvard MD-PhD MSTP Program
[7]Department of Pediatrics
[8]Department of Neurology
[9]Department of Genetics
Harvard Medical School, Boston, MA 02115, USA
[10]Pediatric Neurology Unit, Department of Neurology, Massachusetts General Hospital, Boston, MA 02114, USA
[11]Program in Medical and Population Genetics, Broad Institute of MIT and Harvard University, Cambridge, MA 02142, USA
[12]Clinical and Metabolic Genetics Division, Department of Pediatrics, Hamad Medical Corporation, Doha, 3050, Qatar
[13]Department of Pediatrics, Faculty of Medicine and Health Sciences, United Arab Emirates University, Al-Ain, United Arab Emirates
[14]Department of Genetics
[15]Department of Medical Genetics
King Faisal Specialist Hospital and Research Centre, Riyadh 11211, Saudi Arabia
[16]Department of Anatomy and Cell Biology, College of Medicine, Alfaisal University, Riyadh 11533, Saudi Arabia
[17]Department of Pharmacognosy, College of Pharmacy, King Saud University, Riyadh 11451, Saudi Arabia
[18]Department of Biochemistry and Biophysics, Cardiovascular Research Institute, University of California, San Francisco, San Francisco, CA 94158, USA
[19]Institute of Medical Biology, Human Genetics and Embryology Laboratory
[20]Institute of Molecular and Cellular Biology
A*STAR, Singapore 138648, Singapore
[21]Department of Genetic Medicine and Development, Geneva University, Geneva 1211, Switzerland
[22]Department of Paediatrics, National University of Singapore, Singapore 119260, Singapore
[23]Department of Paediatrics, Faculty of Medicine, University of Jordan, Amman, 11942, Jordan
[24]Co-senior author
*Correspondence: harris@genetics.med.harvard.edu (M.P.H.), bruno@reversade.com (B.R.), christopher.walsh@childrens.harvard.edu (C.A.W.)
http://dx.doi.org/10.1016/j.neuron.2014.12.017

SUMMARY

Katanin is a microtubule-severing complex whose catalytic activities are well characterized, but whose in vivo functions are incompletely understood. Human mutations in *KATNB1*, which encodes the noncatalytic regulatory p80 subunit of katanin, cause severe microlissencephaly. Loss of *Katnb1* in mice confirms essential roles in neurogenesis and cell survival, while loss of zebrafish *katnb1* reveals specific roles for katnin p80 in early and late developmental stages. Surprisingly, *Katnb1* null mutant mouse embryos display hallmarks of aberrant Sonic hedgehog signaling, including holoprosencephaly. *KATNB1*-deficient human cells show defective proliferation and spindle structure, while *Katnb1* null fibroblasts also demonstrate a remarkable excess of centrioles, with supernumerary cilia but deficient Hedgehog signaling. Our results reveal unexpected functions for *KATNB1* in regulating overall centriole, mother centriole, and cilia number, and as an essential gene for normal Hedgehog signaling during neocortical development.

INTRODUCTION

Although human genetics has identified essential roles for many centriole- and cilia-related proteins during human development, the functional relationships between these two crucial organelles are less well understood. Mutations in genes encoding centrosomal proteins cause a wide range of syndromes, notably

microcephaly, which is characterized by reduced brain size with or without other features, such as reduced somatic size. Microcephaly-associated mutations in genes encoding centrosomal and pericentriolar proteins, including *MCPH1*, *CDK5RAP2*, *ASPM*, *CENPJ*, *WDR62*, *CEP152*, *CASC5*, *STIL*, *CEP135*, *CEP63*, *NIN*, *PCNT*, and *POC1A*, implicate a centrosomal pathway important during human neurogenesis (Hu et al., 2014; Mahmood et al., 2011; Thornton and Woods, 2009). However, cellular mechanisms by which centrioles control neurogenesis are still unclear.

A second class of diseases, broadly termed "ciliopathies," manifest with a range of features, but common themes include retinal disease, left-right asymmetry defects, polydactyly, hepatobiliary disease, renal cysts, and obesity (Hildebrandt et al., 2011). These diseases reflect functions of cilia in a wide range of cellular processes, including mechanosensation, chemosensation, and developmental responses to patterning signals and growth factors (Nigg and Raff, 2009; Novarino et al., 2011; Oh and Katsanis, 2012).

Although cilia and centrosomes both function centrally in neocortical development, their interrelationships in the context of neurogenesis are not well understood. The neocortex is formed from a layer of neuroepithelial cells that divide and expand to form radial glial progenitors, which subsequently give rise to intermediate progenitors and, ultimately, neurons (Greig et al., 2013; Lui et al., 2011). Neuronal progenitors lining the lateral ventricle protrude apical primary cilia to receive critical cues from the cerebrospinal fluid, such as IGF2 and Sonic hedgehog (Shh), in order to maintain proliferative cell divisions (Lehtinen et al., 2011; Saade et al., 2013; Tong et al., 2014). Mutations that impair the function of the cilium disrupt progenitor polarity and neurogenesis (Higginbotham et al., 2013; Lee and Gleeson, 2011; Willaredt et al., 2008). Recently, the ciliary membrane and a ciliary remnant have been shown to remain tightly associated with the mother, or older, more mature centriole in dividing apical neuroepithelial cells. The asymmetrical inheritance of both the mother centriole and this apical ciliary membrane allows asymmetrical cilium outgrowth and maintenance of apical stem cells (Paridaen et al., 2013; Wang et al., 2009). These data suggest that relationships between mother centrioles and cilia are crucial to neurogenesis and the maintenance of stem cell character.

Here, we describe recessive mutations in *KATNB1*, encoding the p80 subunit of the microtubule-severing enzyme katanin, that cause severe microcephaly with simplification of cortical gyri and sulci, or microlissencephaly. By modeling the condition in mice and zebrafish, we find that katanin p80 is a crucial regulator of early embryonic development. Remarkably, *KATNB1*-deficient cells show abnormalities of both the centriole and primary cilium. In mouse embryonic fibroblasts (MEFs), loss of katanin p80 leads to the formation of supernumerary centrioles capable of forming multipolar spindles and nucleating ectopic cilia. Evidence of perturbed Shh signaling further supports disruption of ciliary function. Our data provide a new mechanism of microcephaly that involves katanin p80-mediated regulation of interactions between centriole and ciliary signaling.

RESULTS

Mutations in *KATNB1* Cause Microlissencephaly

Three unrelated Middle Eastern families presented with individuals affected with severe microcephaly, global developmental delay, and seizures. MRI of the affected individuals revealed dramatically reduced brain size and cortical volume with simplified gyri, shallow sulci, and enlarged lateral ventricles posteriorly (Figure 1A), with relative sparing of the midbrain, basal ganglia, and cerebellum. Affected individuals also displayed mild facial dysmorphisms and sloping foreheads, consistent with reduced cranial volume (see Figure S1A available online).

Family 1 is a large Jordanian family with five affected individuals from related, consanguineous nuclear families; siblings of the affected individuals are all reported to be healthy (Figure 1B). Family 2 originates from Saudi Arabia, and the affected male proband is the third child of healthy, first-cousin parents (Figure 1B′), with two healthy older siblings. Family 3 is of Palestinian origin, and the affected individual is the fourth child of two healthy parents with no reported consanguinity (Figure 1B″). A sibling of Proband 3 died from a viral illness at age 2, while other siblings are healthy. Several paternal first cousins were reported to display a similar microcephaly and seizure phenotype, although medical records and DNA samples were unavailable.

Medical genetic and neurological evaluation of the affected individuals at birth and throughout life revealed dramatically reduced head circumference, disproportionate to height and weight (Figures S1B–S1D). Detailed clinical information on all affected individuals is available in Table S1. The severely reduced brain size, simplified gyri and enlarged ventricles, especially posteriorly, and relative sparing of the brain stem and cerebellum seen on MRI in affected individuals from all three families bear a striking resemblance to the microlissencephaly caused by mutations in *NDE1* (Alkuraya et al., 2011; Bakircioğlu et al., 2011), and so we use the same term henceforth.

The consanguineous pedigrees implicated recessive inheritance of rare, pathogenic variants. To identify the causative mutations in these families, we undertook a combination of homozygosity mapping, whole-exome sequencing, and targeted next-generation sequencing (see Experimental Procedures for further details). In Family 1, mapping of shared regions that are homozygous and identical-by-descent (IBD) in the affected individuals, and exclusion of common homozygous segments shared by unaffected family members, identified a single shared IBD candidate locus totaling 9 Mb on Chromosome 16 (Figure S1E). Subsequent whole-exome sequencing of Proband 1 revealed a single, unique homozygous variant present in the region of IBD. Whole-exome sequencing in Proband 2 identified 3 homozygous, rare, protein-altering variants, and targeted sequencing of coding exons within blocks of homozygosity greater than 2 cM in Proband 3 identified seven homozygous, rare, protein-altering variants. Crossreferencing all three families identified homozygous deleterious mutations in a single, overlapping gene, *KATNB1*. Sanger sequencing confirmed precise familial segregation of disease-associated variants (Figures S1F–S1F″), and all three variants were absent from European or ethnically matched control populations.
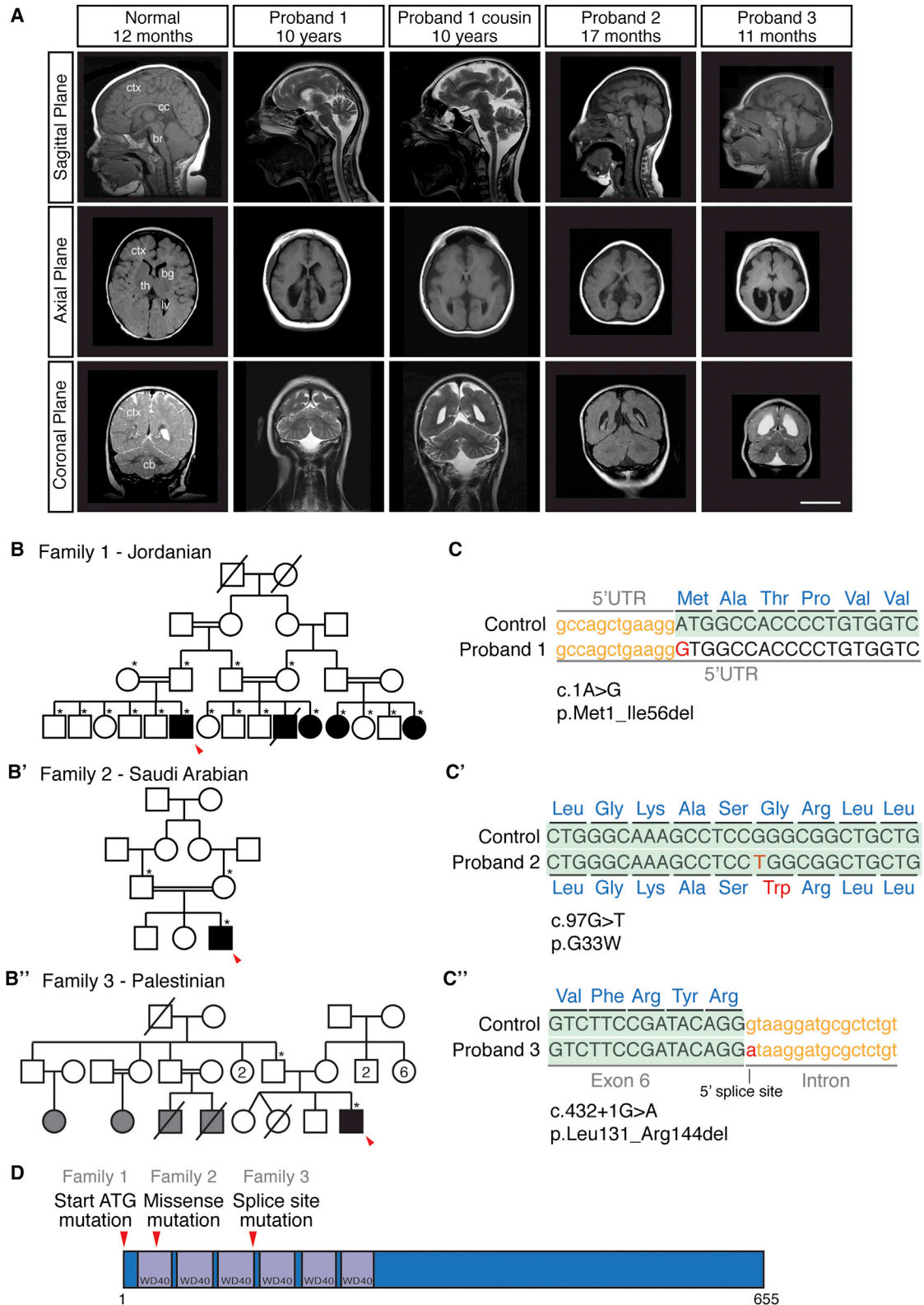
Figure 1. Mutations in *KATNB1* Cause Microlissencephaly

(A) MRI images of affected individuals show reduced cortical size (ctx), simplification of gyral folding pattern, enlarged lateral ventricles (lv) posteriorly and thinning of the corpus callosum (cc), with relative sparing of the cerebellum (cb), basal ganglia (bg), thalamus (th), and brainstem (br). Scale bar, 50 mm.

(legend continued on next page)

KATNB1 encodes the p80 subunit of katanin, a microtubule-severing enzyme comprised of a p60 catalytic subunit and a p80 regulatory subunit (McNally and Vale, 1993). Family 1 carries a mutation that abolishes the initiator ATG codon (Figure 1C), predicted to result either in complete loss of protein, or potential production of an N-terminally truncated protein from a downstream conserved in-frame methionine at position 57. Family 2 carries a missense mutation that converts a highly conserved glycine to a tryptophan (Figure 1C′). Family 3 carries a splice site mutation at the exon-intron boundary of exon 6 that is predicted to abolish all splice donor activity (Figure 1C″), as the first base pair of the splice donor site is 100% conserved in eukaryotes (Mount, 1982; Senapathy et al., 1990). Katanin p80 contains six WD40 repeats in the N terminus of the protein, and the mutations in Families 2 and 3 are located within the first and third WD40 repeats, respectively (Figure 1D). The predicted N-terminal truncated product in Family 1 also disrupts the WD40 domains.

KATNB1 DNA and protein sequences are highly evolutionarily conserved. Using several different methods of model averaging (Zhang et al., 2006), we calculated nonsynonymous to synonymous substitution ratios (Ka/Ks) between 0.03 and 0.08, indicating extremely strong negative selection of nonsynonymous variation. The specific proband nucleotide mutation sites are also highly conserved, with GERP scores of 4.97, 4.28, and 5.01 and for the start codon, missense, and splice site mutation sites, respectively (Cooper et al., 2005; Davydov et al., 2010). Additionally, for the missense mutation, comparing the MultiZ alignment across 100 vertebrate species, all but one species contain glycine at that residue (Blanchette et al., 2004; Karolchik et al., 2014). Together, these data indicate that the *KATNB1* gene and the proband mutation sites are extremely well conserved, and that mutation of these sites is most likely pathogenic.

Mutations in *KATNB1* Alter mRNA Splicing and Protein Quantity

The high conservation of *KATNB1* and the highly conserved protein structure of WD40 repeats (Neer et al., 1994) suggest that the identified mutations would severely disrupt katanin p80 protein stability and function. Expression studies in primary fibroblasts and induced pluripotent stem cells (iPSCs) derived from Proband 1 identified reductions in both katanin p80 and p60 in human cells. The start codon mutation causes the loss of the first methionine, and translation is predicted to initiate at the next in-frame methionine 56 amino acids downstream (Figure S2B). *KATNB1* and *KATNA1* mRNA are detectable at comparable levels in Proband 1-derived iPSCs compared to control cell lines by quantitative RT-PCR (Figure 2A). However, full-length katanin p80 is not detectable in Proband 1-derived primary fibroblasts or iPSCs, and in iPSCs we find a new, smaller katanin p80 protein product consistent with the predicted N-terminal truncated

form (Figure 2B). Remarkably, p60 protein was also undetectable in primary fibroblasts and greatly reduced in iPSCs despite unchanged transcript levels (Figures 2A and 2B), most likely resulting from a posttranscriptional event. A lymphoblastoid cell line derived from Proband 2 showed an 84% reduction in katanin p80 protein compared with a control line, with protein minimally detectable after long exposure (Figure 2C), suggesting that the missense allele is either null, due to defective function of the mutant protein, or hypomorphic, with some residual protein and residual activity. Interestingly, we also find a concomitant 64% decrease of the katanin p80 binding partner katanin p60 in Proband 2-derived lymphoblasts, compared with control (Figure 2C), suggesting that the loss of katanin p80 impairs katanin p60 stability.

For Family 3, we analyzed mRNA splicing using a minigene comprised of full-length cDNA, including the introns immediately upstream and downstream of the splice mutation site (Figure 2D). We transfected tagged wild-type and mutated Proband 3 minigene constructs into HEK293T cells, followed by RT-PCR, and found that, compared with wild-type, the mutant minigene creates a smaller RNA product corresponding to skipping of exon 6 (dele6, Figure 2E). Sanger sequencing of the RT-PCR product identified the presence of the exon 5–exon 7 boundary (Figure 2F). Expression studies showed that the splicing mutation results in stable, albeit functionally defective, protein. Transfection of tagged wild-type and Proband 3 minigenes, and wild-type and exon 6-deleted (dele6) cDNAs, into HEK293T cells with quantitative western blot revealed a 51%–77% reduction in katanin p80 from the mutant minigene and cDNAs compared with their wild-type counterparts (Figure 2G). Because exon 6 is an in-frame exon, and mutant protein is present at lower quantities than wild-type, this mutant form may be hypomorphic. Whereas tagged, wild-type katanin p80 localizes to the centrosome of interphase cells (Figure 2H), most tagged dele6 protein accumulates in the nucleus during interphase, with minimal localization to the centrosome (Figure 2H), indicating that the misspliced protein is functionally perturbed. In summary, all three mutations disrupt the N-terminal WD40 repeats of KATNB1, result in lower levels of katanin p80 as well as p60 protein, yet have the potential to produce defective proteins with some partial function.

Katanin p80 Is Required for Embryonic Survival

To study functions of katanin p80 in vivo, we generated a *Katnb1* gene-trap (gt) mouse line, with the gene-trap vector inserted between coding exons 2 and 3 (Figure 3A). We confirmed by RT-PCR that *Katnb1* coding exon 2 splices fully to the Engrailed-2 splice acceptor of the gene-trap vector, with no detectable wild-type *Katnb1* mRNA in homozygous gene-trap mutants (Figures 3B and 3C). Katanin p80 protein is reduced by 51% in heterozygous embryos and is undetectable in

(B–B″) Pedigrees of families with microlissencephaly. Square, male; circle, female; red arrowhead, affected proband; black shading, affected individual; gray shading, reported affected individual, medical records unavailable; double lines, consanguineous marriages; diagonal line, deceased; asterisk, DNA sample collected.

(C–C″) Mutation in Family 1 abolishes start ATG codon. Mutation in Family 3 is at a 5′ splice site. Missense mutation in Family 2 converts a conserved glycine to a tryptophan.

(D) Predicted protein structure of katanin p80. Mutations lie at first amino acid and in WD40 domains.

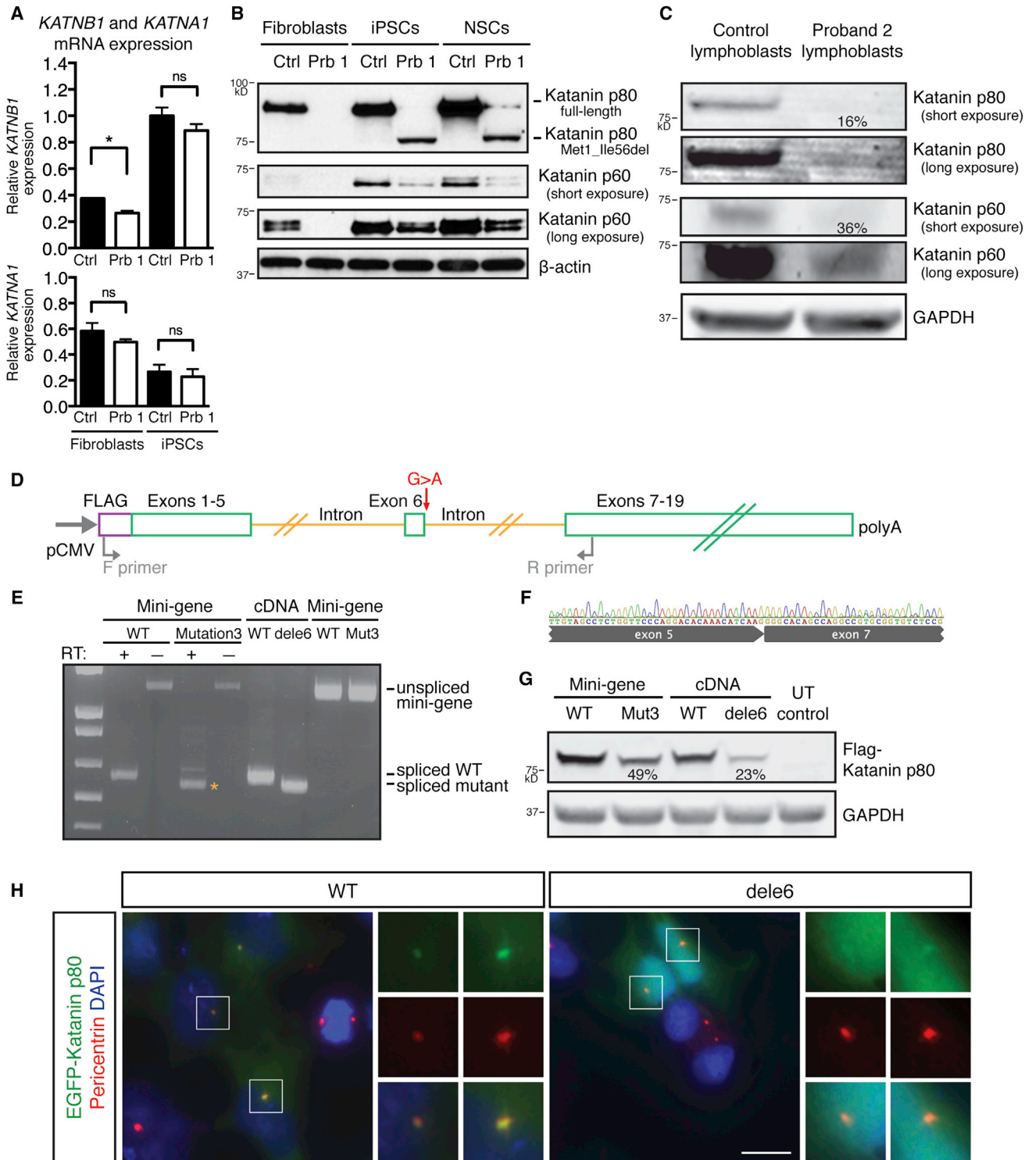See also Figure S1, Table S1, and Movie S1.

Figure 2. Mutant *KATNB1* Alleles Produce Less Protein Than Wild-Type Alleles, and dele6 Mutant Protein Is Mislocalized

(A) qRT-PCR of Proband 1-derived fibroblast and iPSC lines shows presence of *KATNB1* and *KATNA1* mRNA at levels comparable to control cell lines. Unpaired t test, p < 0.05; ns, not statistically significant.

(B) Western blot of Proband 1-derived fibroblast and iPSC lines shows absence of full-length katanin p80 and presence of smaller protein product compared to control (top). Katanin p60 levels are also reduced (bottom).

(C) Western blot of Proband 2-derived lymphoblastoid cell lines shows near absence of katanin p80, detectable only at high exposure (top), and reduction of katanin p60 (bottom). Quantification using LI-COR imaging system.

(legend continued on next page)

homozygous mutant embryos (Figure 3D), indicating that the gene-trap allele is almost certainly null. Similar to our primary human cell line data (Figures 2B and 2C), katanin p60 protein levels are reduced by 39% and 72% in the heterozygous and homozygous Katnb1 gene-trap embryos, respectively (Figure 3E).

Homozygous null Katnb1 gene-trap embryos die embryonically, with dramatically reduced body size by embryonic day 15.5 (E15.5) (Figures 3F and 3G). Embryos are found along a spectrum of phenotypic severity, and some very severely affected embryos die as early as E12.5. All homozygous mutant embryos are grossly morphologically abnormal, with features including pallor of the liver, microophthalmia to anophthalmia, and reduced limb bud outgrowth (Figure 3H). In addition, homozygous mutant embryos show forebrain abnormalities ranging from microcephaly to holoprosencephaly, in which the two hemispheres of the brain fail to separate, resulting in a single ventricle (Figures 3H–3J). Histopathological analysis of the embryos revealed a lack of red blood cells in the liver, suggesting failed definitive erythropoiesis, which is a potential cause of embryonic death (data not shown) (Baron, 2013). Underdeveloped limb buds, anophthalmia, and holoprosencephaly are commonly seen in mouse mutants with defective Shh signaling (Chiang et al., 1996; Hayhurst and McConnell, 2003; Litingtung et al., 2002) and are associated with human mutations in SHH (Belloni et al., 1996; Roessler et al., 1996), while Indian hedgehog, another hedgehog family protein, has been implicated in definitive erythropoiesis (Cridland et al., 2009). The overlap of phenotypes between homozygous Katnb1 gene-trap mice and Shh pathway mutants raises the unexpected possibility that katanin p80 might be involved in modulating Shh signaling. These data indicate that katanin p80 is required for embryonic development and survival, and confirm the association of the human mutations with the severe brain malformations.

Katanin p80 Is Required for Early Embryogenesis and Formation of Anterior Structures in Zebrafish

As a second, independent model of katanin loss of function during development, we utilized the high conservation of the katanin p80 protein sequence and gene structure in zebrafish (Figures 4A and S3A) and targeted the exon 6-intron 6 boundary near the Proband 3 mutation site with TALEN endonucleases (Figure 4B; Table S2). We generated a series of mutant alleles harboring different frameshift as well as in-frame deletions and insertions at the target site (Figures 4B and S3B). Most of the alleles are frameshift mutations and are predicted to lead to early termination and, consequently, truncated proteins (Figure 4C and S3B).

Mutant progeny from F1 carriers of truncated alleles are viable. However, progeny of females deficient for katnb1, although able to develop through 70% epiboly, show a wide spectrum of phenotypes stemming from defects in gastrulation and formation of anterior structures, ranging from milder microcephaly to more severe anencephaly and early embryonic death (Figures 4D, 4E, and S3C). The similar phenotypic results observed in mice and zebrafish deficient for Katnb1 demonstrate that katanin plays a major role during early embryogenesis and patterning of anterior structures. Since the humans we identified with KATNB1 mutations survive beyond birth into childhood, the embryonic lethality of Katnb1 deficiencies suggests that the three identified human alleles may retain partial function. Interestingly, the maternal rescue observed in the zebrafish (Figure 4E) indicates that normal maternal katnb1 mRNA is sufficient to permit generally normal growth and patterning during postembryonic development in the absence of zygotic katnb1, suggesting that variation in developmental timing of katanin p80 function also affects phenotypic severity.

Katnb1 Is Ubiquitously Expressed in the Brain and Critical for Neocortical Development

Given the striking brain morphological phenotypes in the probands and homozygous gene-trap mouse embryos, we investigated functions of katanin p80 during cortical development. Katanin p80 is expressed in the mouse cerebral cortex throughout development (Figure 5A). To evaluate cell-type-specific expression, we took advantage of the presence of a LacZ cassette in the gene-trap vector and stained for LacZ protein in the neocortex of heterozygous embryos. We found ubiquitous staining throughout the proliferative ventricular zones and in the cortical plate (Figure 5B), in agreement with available mouse transcriptome data (Ayoub et al., 2011).

The dramatic reduction in brain size seen in homozygous mutant mice reflects abnormal proliferation as well as cell death. Following a pulse of bromodeoxyuridine (BrdU) to pregnant dams at E12.5, a stage corresponding to early neurogenesis, we find a 35% reduction in number of actively proliferating cells in homozygous mutant embryos compared with wild-type, confirming that fewer cycling progenitors are indeed present (Figures 5C and 5D). Furthermore, we find that overall cortical thickness is reduced by 54% at E13.5, a stage corresponding to peak neurogenesis (Figures 5E–5H), with preserved cell polarity (Figure S5A). To more specifically characterize cortical defects, we performed immunohistochemistry for specific progenitor subtypes and neurons. Sox2 immunoreactivity, which identifies radial neuroepithelial progenitors, is reduced 32% in Katnb1 null embryos. Tbr2 immunoreactivity, which identifies intermediate progenitors formed by asymmetric divisions of radial neuroepithelial cells, is reduced more severely, with 72% depletion. Neurons, labeled with DCX immunoreactivity and derived

(D) Schematic of the splice site minigene cDNA construct. Primer arrows show location of PCR primers for (E).
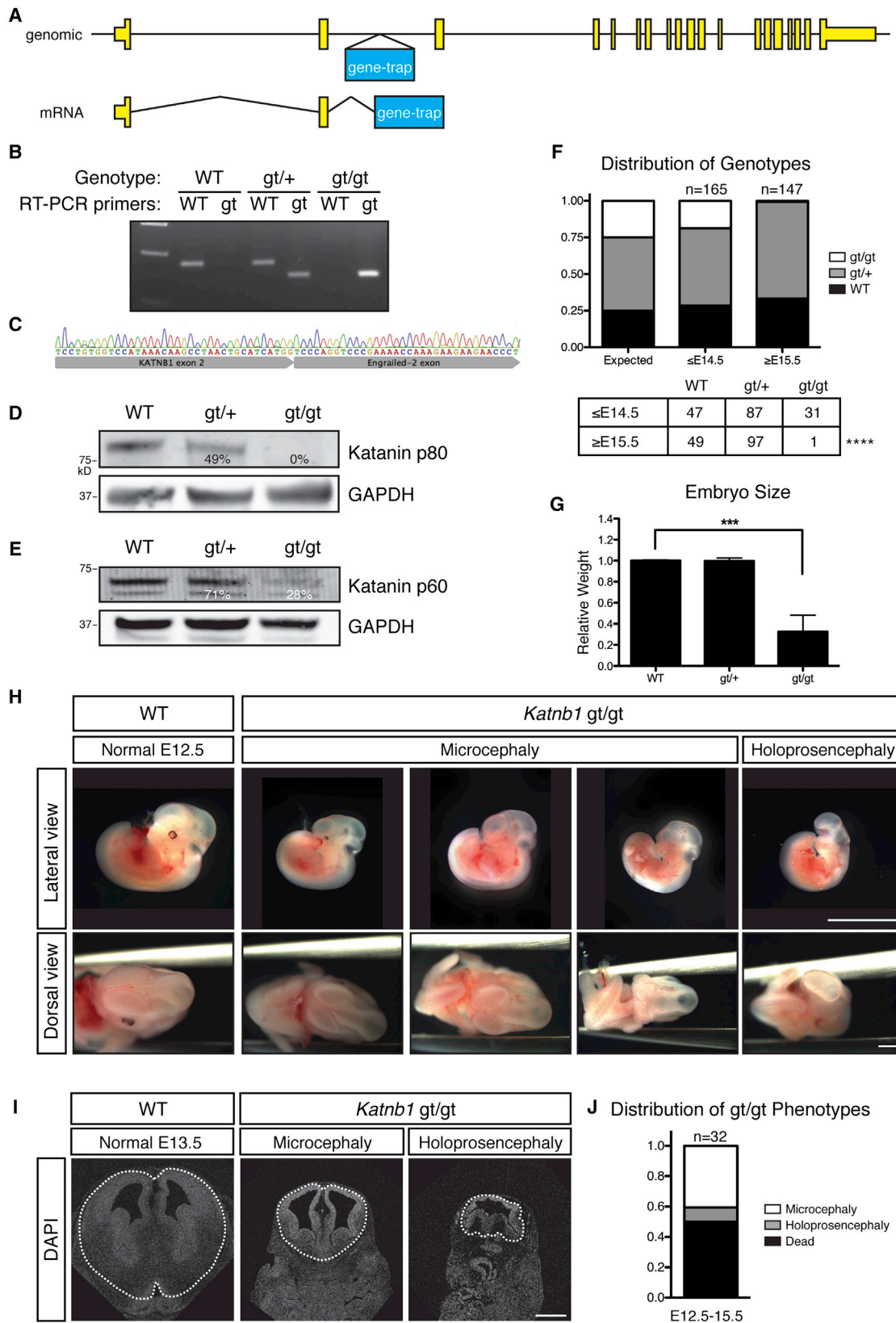
(E) RT-PCR results of minigene assay. Smaller product in splice mutant minigene (asterisk) corresponds in size to deletion of exon 6 (dele6).

(F) Sanger sequencing of smaller spliced product (asterisk in E) confirms skipping of exon 6.

(G) Western blot of transfected minigenes and cDNAs shows reduced protein levels in splice mutant allele relative to wild-type. Quantification using the LI-COR imaging system.

(H) Wild-type EGFP-tagged katanin p80 localizes to the centrosome (left; Pericentrin), but EGFP-tagged dele6 mutant protein diffuses throughout the nucleus, with minimal centrosomal localization (right). Scale bar, 10 um.
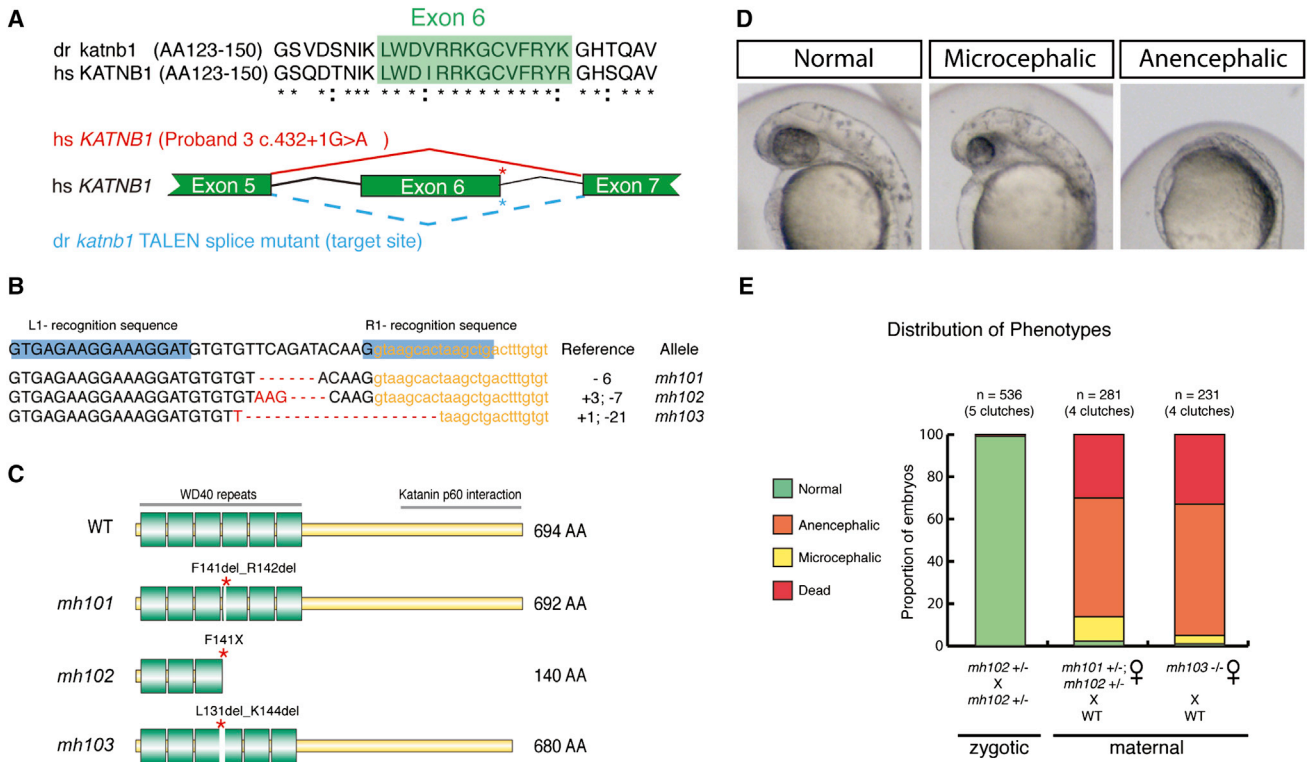
See also Figure S2.

A genomic / mRNA gene-trap

B

Genotype:	WT		gt/+		gt/gt	
RT-PCR primers:	WT	gt	WT	gt	WT	gt

C

TCCTGTGGTCCATAAACAAGCCTAACTGCATCATGGTCCCAGGTCCCGAAAACCAAAGAAGAAGAACCCT

KATNB1 exon 2 / Engrailed-2 exon

D

	WT	gt/+	gt/gt	
75-kD		49%	0%	Katanin p80
37-				GAPDH

E

	WT	gt/+	gt/gt	
75-		71%	28%	Katanin p60
37-				GAPDH

F Distribution of Genotypes

n=165   n=147

gt/gt ☐, gt/+ ▨, WT ■

Expected   ≤E14.5   ≥E15.5

	WT	gt/+	gt/gt	
≤E14.5	47	87	31	
≥E15.5	49	97	1	****

G Embryo Size

***

Relative Weight

WT   gt/+   gt/gt

H

	WT	*Katnb1* gt/gt			
	Normal E12.5	Microcephaly			Holoprosencephaly
Lateral view					
Dorsal view					

I

	WT	*Katnb1* gt/gt	
	Normal E13.5	Microcephaly	Holoprosencephaly
DAPI			

J Distribution of gt/gt Phenotypes

n=32

Microcephaly ☐, Holoprosencephaly ▨, Dead ■

E12.5-15.5

(legend on next page)

Figure 4. Maternal Contribution of *katnb1* Is Essential for Zebrafish Gastrulation

(A) Katanin p80 protein and gene structure is highly conserved between humans and zebrafish.

(B) TALENs targeting the genomic region surrounding the zebrafish *katnb1* exon 6-intron 6 boundary create a series of mutant alleles. Reference sequence (top). Blue box, TALEN recognition sites; dash, deleted base pairs; red letters, inserted base pairs.

(C) Mutant alleles are predicted to alter protein structure by deletion of amino acids or early truncation of katanin p80 protein.

(D) Progeny of mutant females show a wide spectrum of phenotypes, ranging from early embryonic lethality and anencephaly to microcephaly.

(E) Maternal effect of *katnb1* is observed in crosses of mutant females, compared with progeny arising from heterozygous carriers. Embryos developed normally until 70% epiboly.

See also Table S2 and Figure S3.

from asymmetrical divisions of radial neuroepithelial cells or from the Tbr2-positive progenitors, are the most severely affected, with an 83% reduction compared to wild-type (Figures 5E–5H). These results reveal a striking reduction in cycling ventricular zone progenitors in *Katnb1* null cortex, but an even more profound loss of cells that depend upon asymmetrical cell divisions, including intermediate progenitors and neurons. These data parallel the results of katanin p80 loss in the *Drosophila* brain presented in an accompanying paper, in this issue of *Neuron* (Mishra-Gorur et al., 2014). We hypothesized that cell death might also be a factor in neuronal depletion, and indeed we find apoptotic cells, marked by activated cleaved caspase 3, in

Figure 3. *Katnb1* Gene-Trap Mutants Die by E14.5, with Brain Phenotypes Ranging from Microcephaly to Holoprosencephaly

(A) Location of gene-trap insertion. Gene-trap insertion leads to early truncation of *Katnb1* mRNA, to mimic a null allele.

(B and C) RT-PCR confirms absence of wild-type allele in homozygous gene-trap mice (B). Sanger sequencing of gene-trap RT-PCR product confirms splicing of exon 2 into gene-trap cassette (C).

(D and E) Katanin p80 protein is absent in gt/gt mice (D), and less katanin p60 protein is produced in gt/gt mice, compared with wild-type (E). Quantification using the LI-COR imaging system.

(F) Homozygous gt/gt mice are present in expected Mendelian ratios before E14.5 but are almost never found after E15.5, indicating that *Katnb1* loss of function is embryonically lethal. Chi-square test, p < 0.0001.

(G) Compared with wild-type, homozygous gt/gt embryos are dramatically reduced in body size at E14.5. Error bars indicate mean ± SEM. One-way ANOVA, p < 0.001.

(H) Homozygous gt/gt embryos vary in size, with brain phenotypes ranging from microcephaly (embryos 2–4) to holoprosencephaly (embryo 5). Some homozygous gt/gt embryos are micropthalmic (embryo 2), while others have no eye development (embryos 3–5), and all have underdevelopment of the limb buds and pallor of the liver. All pictured embryos are littermates. Scale bar, 5 mm (top) and 1 mm (bottom).

(I) Coronal sections through embryonic brains show reduced cortical size, thickness, and holoprosencephaly in homozygous gt/gt embryos. Dashed line, outline of brain. Scale bar, 200 um.

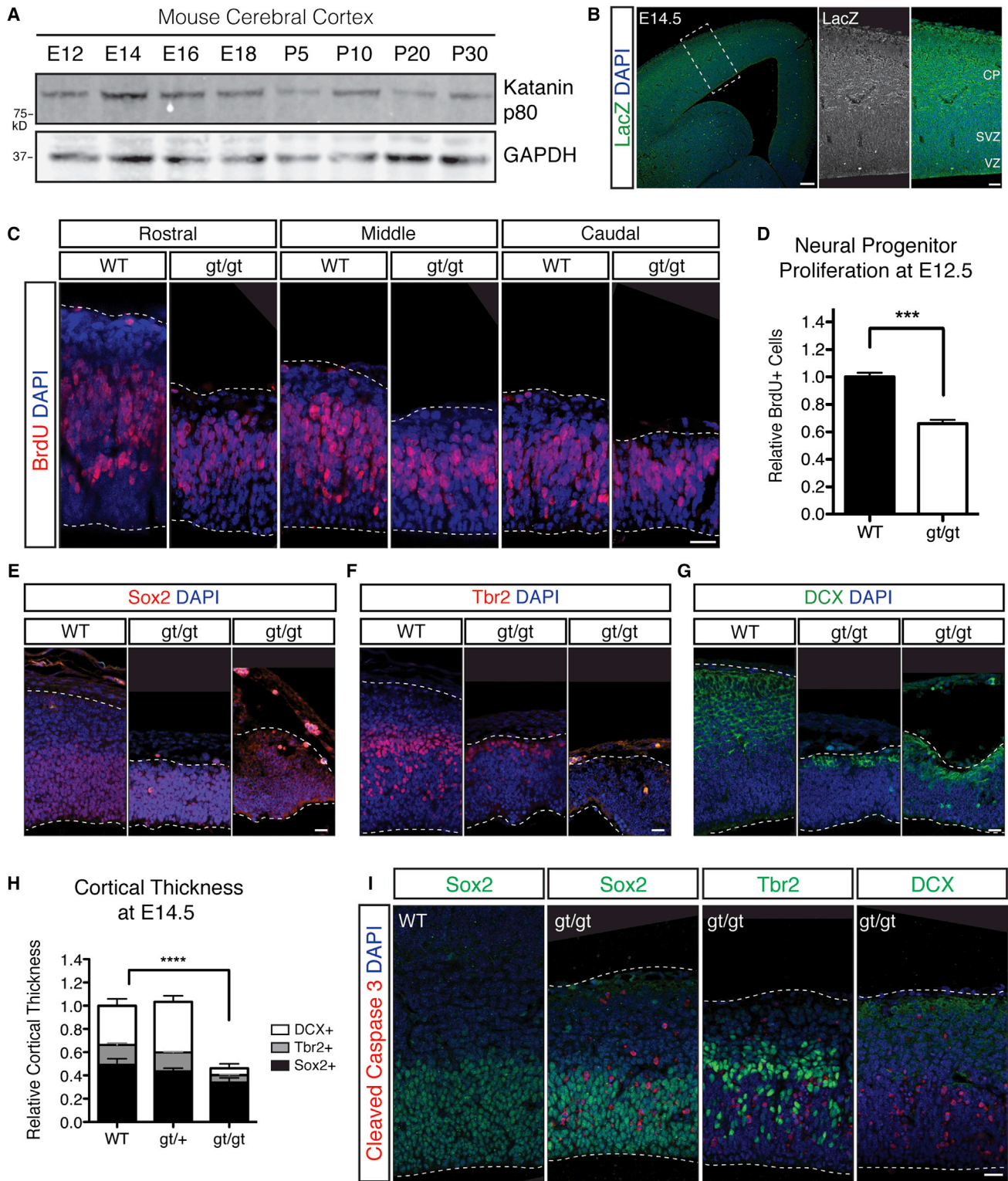(J) Distribution of homozygous gt/gt phenotypes recovered between E12.5 and E15.5.

Figure 5. Loss of Katanin p80 Impairs Proliferation of Cortical Progenitors at E12.5, with Fewer Progenitors and Postmitotic Neurons Present in Cortex

(A) Katanin p80 protein is present in the cerebral cortex throughout embryonic and postnatal development.

(B) Katanin p80 protein is present throughout the developing cortex at high levels in postmitotic neurons in the cortical plate, and lower levels in progenitors of the ventricular and subventricular zones at E14.5. VZ, ventricular zone; SVZ, subventricular zone; CP, cortical plate. Scale bar, 50 um (left) and 20 um (inset, right).

(legend continued on next page)

homozygous mutant brains. Even in the most mildly affected homozygous gene-trap embryos, apoptosis is abundant throughout the brain, particularly in the proliferative ventricular zones of the cortex, whereas apoptotic cells are absent from wild-type brains (Figure 5I). We obtained similar results using neural stem cells (NSCs) differentiated from human iPSCs. Proband 1-derived neurospheres fail to grow and exhibit widespread apoptosis (Figures S5B–S5D). Together, these data indicate that katanin p80 is required for neuronal progenitor proliferation and survival during cortical development.

Loss of Katanin p80 Disrupts Spindle Structure and Mitosis

To better understand the cellular functions of katanin p80 during human development, we studied proband-derived cell lines. Katanin p80 and p60 localize to the spindle poles of mitotic cells and to the pericentriolar matrix of interphase cells (Figures S5A–S5C). In immortalized human lymphoblasts and human iPSCs expressing mutant *KATNB1* alleles, we find defects in centrosomal structure and function. Approximately 49% of S phase Proband 2-derived lymphoblasts contain more than two centrosomes, compared with 11% in control lymphoblasts (Figures 6A and 6B). Instead of localizing perinuclearly, these centrosomes cluster in the center of the cell, with the DNA arranged around the centrosomes (Figure 6A). iPSCs derived from Proband 1 displayed mitotic abnormalities in 51% of cells, compared to only 4% of control iPSCs: 10% of cells displayed multipolar spindles, with supernumerary chromosomes and excess kinetochores, 22% of cells displayed abnormal monoastral spindles, and an additional 19% contain misaligned chromosomes (Figures 6C and 6D). Flow cytometry analysis for DNA content on lymphoblasts from Proband 2 revealed an increased proportion of cells in S and G2 phase, compared with control lymphoblasts (Figures 6E and 6F), indicative of cell cycle perturbation and aneuploidy.

Katanin p80 Limits Centriole Number

We further investigated centriole biogenesis in MEFs isolated from gene-trap embryos. *Katnb1* null MEFs are more severely affected than proband-derived mutant cell lines, with 76% of gene-trap MEFs containing multipolar mitotic spindles, compared with 12% in wild-type MEFs (Figures 7A and 7D). We also found binucleate homozygous gene-trap MEFs, likely resulting from aneuploid divisions (Shi and King, 2005), while we almost never found binucleate wild-type MEFs (data not shown). MEFs isolated from homozygous gene-trap embryos often failed to proliferate (Figure S6C), and those homozygous gene-trap MEFs that did grow well in vitro divided significantly more slowly than wild-type MEFs (Figure 7F), consistent with the widespread defects in proliferation observed in the mutant embryos.

Defects in cytoskeletal structure in homozygous gene-trap MEFs, with increased acetylated tubulin immunoreactivity around the centrosome (Figure S6D), suggest increased overall microtubule stability. Furthermore, we find more prominent staining for CAMSAP2, a microtubule minus-end protein that protects against depolymerization, as well as more linear, streak-like staining for EB1, a microtubule plus-end protein (Figures S6E and S6F). Together, these data suggest that microtubule dynamics are altered and that loss of katanin p80 results in a more stabilized cytoskeleton.

Surprisingly, we found a high proportion of overduplicated centrioles in homozygous gene-trap MEFs (Figure 7B), with 76% of cells displaying supernumerary centrioles (Figure 7E), consistent with our multipolar spindle data. Transmission electron microscopy of centrosomes reveals that these ectopic centrioles have normal 9-fold symmetry but are unpaired, unlike wild-type, paired centrioles (Figures 7C, S6A, and S6B). These supernumerary centrioles associate with multiple centrosomal proteins, including γ-tubulin, Stil, and Cep63 (Figure 7B), suggesting they form functional centrosomes and may explain the origin of the mitotic spindle defects we observe (Figures 7A and 7D).

Loss of Katanin p80 Causes Supernumerary Cilia and Abrogates Sonic Hedgehog Signaling

The mother centriole is the older centriole in a cell, and normal cells contain only one mother centriole. Examining the localization of two mother centriolar proteins, Ninein and Cep164, revealed the surprising presence of multiple mother centrioles in *Katnb1* homozygous gene-trap MEFs (Figure 8A), suggesting defects in not just centriole number, but also centriole maturation and identity.

Since the mother centriole nucleates the primary cilium, the presence of multiple mother centrioles suggested that *Katnb1* mutant cells may be capable of nucleating multiple cilia. Indeed, after serum starvation to induce cilia growth, we identified many cells with multiple Ift88- or Arl13b-positive cilia (Figure 8B). Over 35% of *Katnb1* homozygous gene-trap MEFs possess supernumerary cilia (Figure 8D), nearly four times as many as wild-type MEFs, confirming an excess of functional mother centrioles in *Katnb1* mutant cells. Some cells contain only a second, shorter cilium, but other cells grow two or even three full-length cilia (Figures 8B and 8D). As with wild-type cells, *Katnb1* mutant MEFs do not produce cilia without serum starvation (data not shown), suggesting that the multiple cilia arise from supernumerary centrioles upon initiation of ciliogenesis, rather than from defective ciliary resorption.

The overproduction of cilia in the absence of katanin p80 raised the question of whether homozygous gene-trap MEFs

(C) Fewer actively proliferating cortical progenitors are labeled by acute BrdU injection at rostral (left), middle (middle), and caudal (right) matched coronal sections in gt/gt cortex compared with wild-type. Scale bar, 20 um.
(D) Quantification of BrdU-positive cells per length of ventricular surface. Error bars indicate mean ± SEM. Unpaired t test, p < 0.001.
(E–G) Homozygous gt/gt mutant cortex is reduced in thickness at E12.5 compared with wild-type, with preferential reduction in intermediate progenitors (F, Tbr2+) and neurons (G, DCX+) over radial glia (E, Sox2+). Scale bar, 20 um.
(H) Quantification of radial thickness of cortex, with percent composition of markers in (E)–(G). Error bars indicate mean ± SEM. One-way ANOVA, p < 0.01.
(I) Apoptotic cells labeled by activated cleaved caspase 3 are abundant in homozygous gt/gt ventricular zones, even in mildly affected embryos. Scale bar, 20 um.
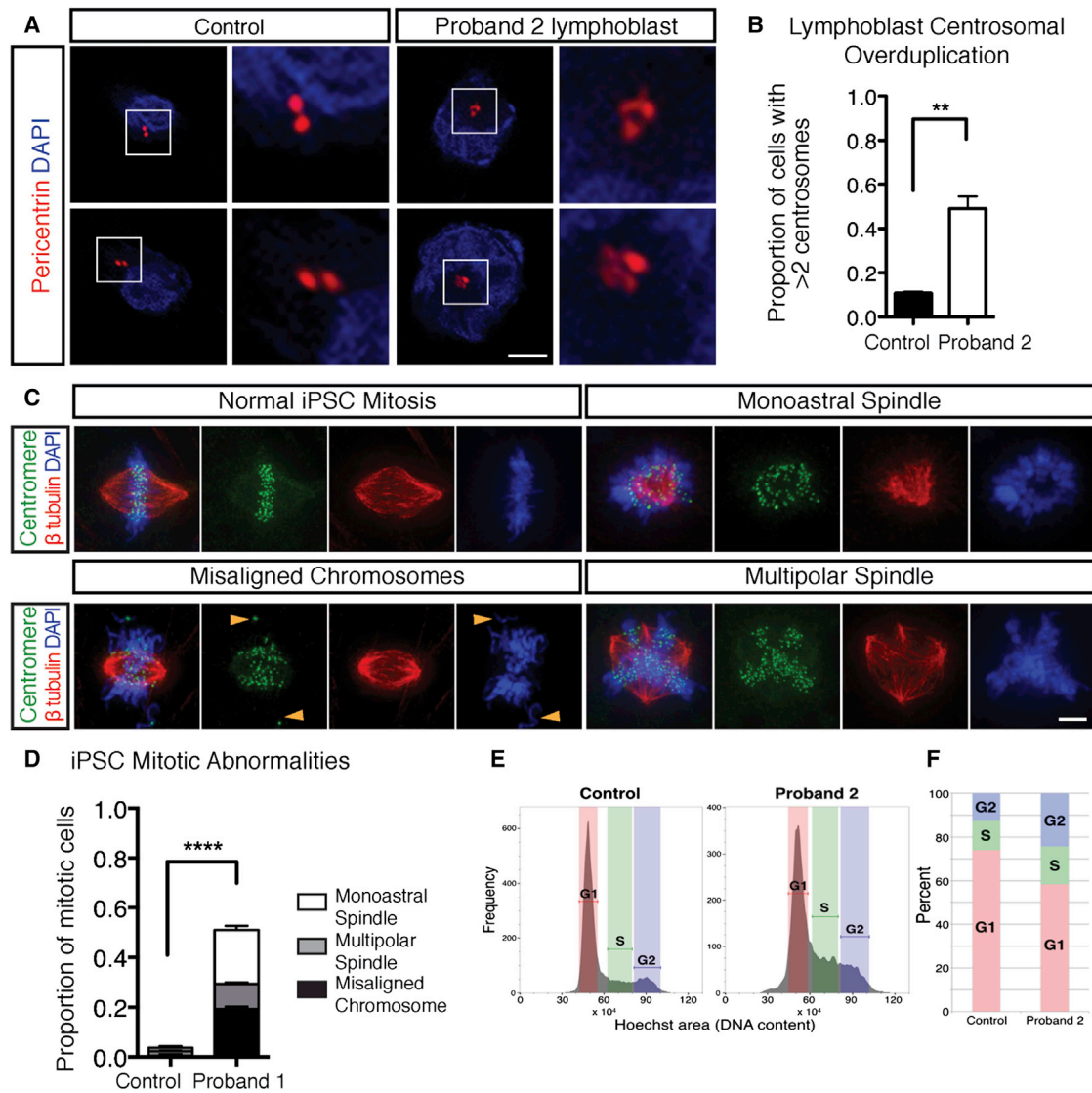See also Figure S4.

Figure 6. Loss of Katanin p80 Causes Centrosome and Centriole Overduplication in Proband-Derived Cell Lines and MEFs

(A) Lymphoblasts derived from Proband 2 undergo centrosomal overduplication, with DNA surrounding centrally located centrosomes. Scale bar, 10 um.

(B) Quantification of proportion of lymphoblasts with overduplicated centrosomes. Unpaired t test, p < 0.01.

(C) Mitotic iPSCs derived from Proband 1 contain monoastral spindles, multipolar spindles, and lagging chromosomes (arrowhead). Scale bar, 10 um.

(D) Quantification of proportion of mitotic iPSCs with abnormal mitoses. Unpaired t test, p < 0.0001.

(E and F) A greater percentage of Proband 2-derived lymphoblasts are aneuploid and have skewed DNA content compared with control lymphoblasts by FACS (E), indicating that the cell cycle is disrupted in proband-derived lymphoblasts (F).

See also Figure S5.

also show alterations in ciliary signaling. The holoprosencephaly seen in homozygous gene-trap embryos suggested a defect in Shh signaling, which, in vertebrates, is dependent on cilia (Huangfu and Anderson, 2005; Huangfu et al., 2003; Mahjoub and Stearns, 2012). We triggered Shh signaling in MEFs using Smoothened agonist (SAG) stimulation. SAG normally causes Gli3 and Smoothened (Smo) to accumulate at the tips of primary cilia. In contrast, Gli3 failed to accumulate in cilia in SAG-stimulated MEFs lacking katanin p80 (Figure 8C), with a 77% reduction in Gli3 localization to the ciliary tip in homozygous

gene-trap MEFs (Figure 8E). Smoothened accumulation in cilia in SAG-stimulated MEFs is also decreased in homozygous gene-trap MEFs, even in cells containing only a single cilium (Figure S7A). qRT-PCR analysis of downstream targets *Gli1* and *Patched1*, which are normally upregulated in response to Shh signaling, showed a 5-fold increase in *Gli1* induction and 11.8-fold increase in *Patched1* induction upon SAG stimulation in wild-type MEFs, but no response in homozygous gene-trap MEFs (Figures 8F and 8G). Together, these data demonstrate that the loss of katanin p80 leads to overduplication of centrioles

and excessive maternal centrioles, leading to supernumerary cilia, and that the resulting multiple cilia fail to properly transduce Shh signals.

DISCUSSION

Here, we identify katanin p80 as a critical regulator of human brain development, and extend its functions beyond regulation of microtubule severing and the mitotic spindle. Three independent mutations in *KATNB1*, affecting protein levels and subcellular localization, result in severe microlissencephaly in humans, and complete genetic ablation of *Katnb1* leads to embryonic lethality in mice and zebrafish. On a cellular level, loss of katanin p80 causes the formation of supernumerary centrioles, including extra mother centrioles. These centrioles result in multipolar spindles and also nucleate supernumerary cilia, leading to reduced Shh signaling. Together, these data implicate katanin as a regulator of mother and daughter centriole number, and of the ciliary number and function that follow, thus greatly expanding our view of katanin function.

Despite the severe microlissencephaly seen in humans with *KATNB1* mutations, the human mutations we identified are most likely hypomorphic. Katanin p80 is essential during early embryogenesis in both mice and zebrafish. Humans do not display phenotypes as extreme as those as seen in the loss-of-function mouse or zebrafish mutants, nor do they show evidence of defects classic for ciliary or Shh dysfunction, such as polycystic kidney disease, laterality defects, midline patterning defects (including holoprosencephaly), or digit anomalies (Dubourg et al., 2007; Hildebrandt et al., 2011; Novarino et al., 2011). Additionally, NSCs derived from human iPSCs do not develop excess cilia or decreased Shh signaling seen in loss-of-function MEFs, further supporting the hypomorphic nature of the human alleles. This may reflect the specific mutations we have identified, all of which disrupt the N-terminal WD40 repeats, and result in reduced, but not completely abolished, protein levels; thus, the mutated proteins may retain enough residual activity to rescue the severe, complete loss-of-function phenotypes. Finally, a previously published mouse carrying a missense mutation in *Katnb1* is viable, with defects observed only in spermatogenesis (O'Donnell et al., 2012), suggesting that alleles of *KATNB1* can give rise to varied phenotypes of altered severity (see also Mishra-Gorur et al., 2014).

Our results also indicate that there are distinct temporal roles for katanin. Loss of maternal *katnb1* results in severe defects of gastrulation, whereas loss of zygotic zebrafish *katnb1* is compatible with survival and growth to viable, fertile adults, indicating that *katnb1* is necessary for tissue patterning during early development, with additional roles during later development. Therefore, the more severe phenotype seen in mice may represent early loss of mammalian katanin p80 function, and the milder human disease phenotypic spectrum may arise from loss of katanin p80 function later during development, possibly in a nervous-system-specific manner.
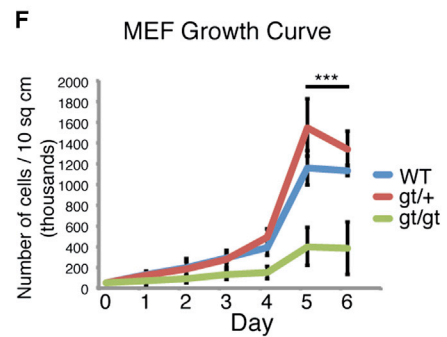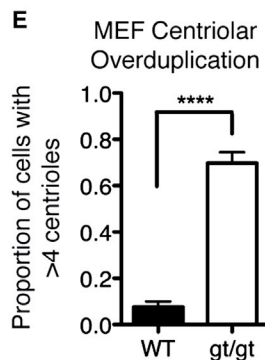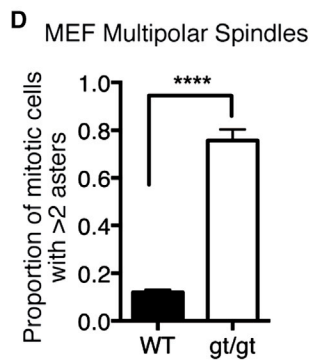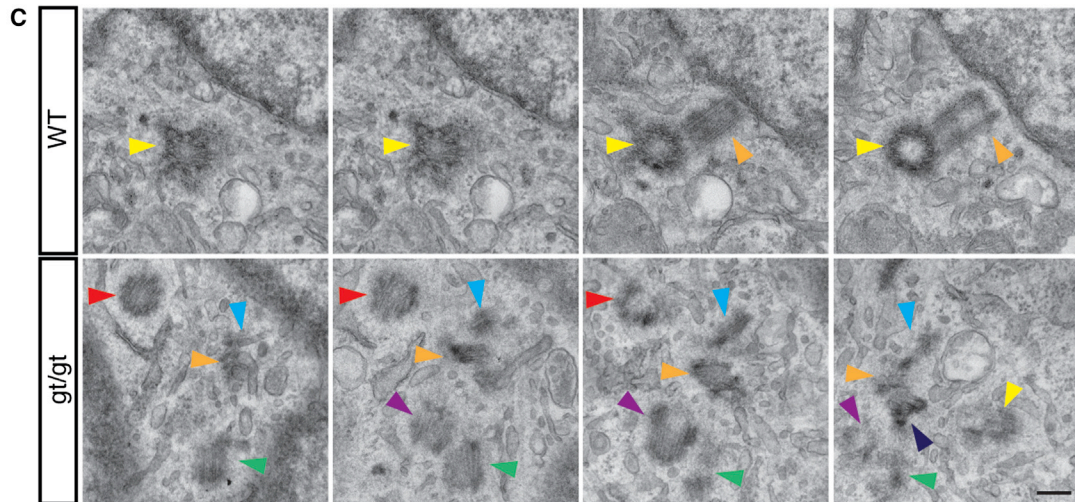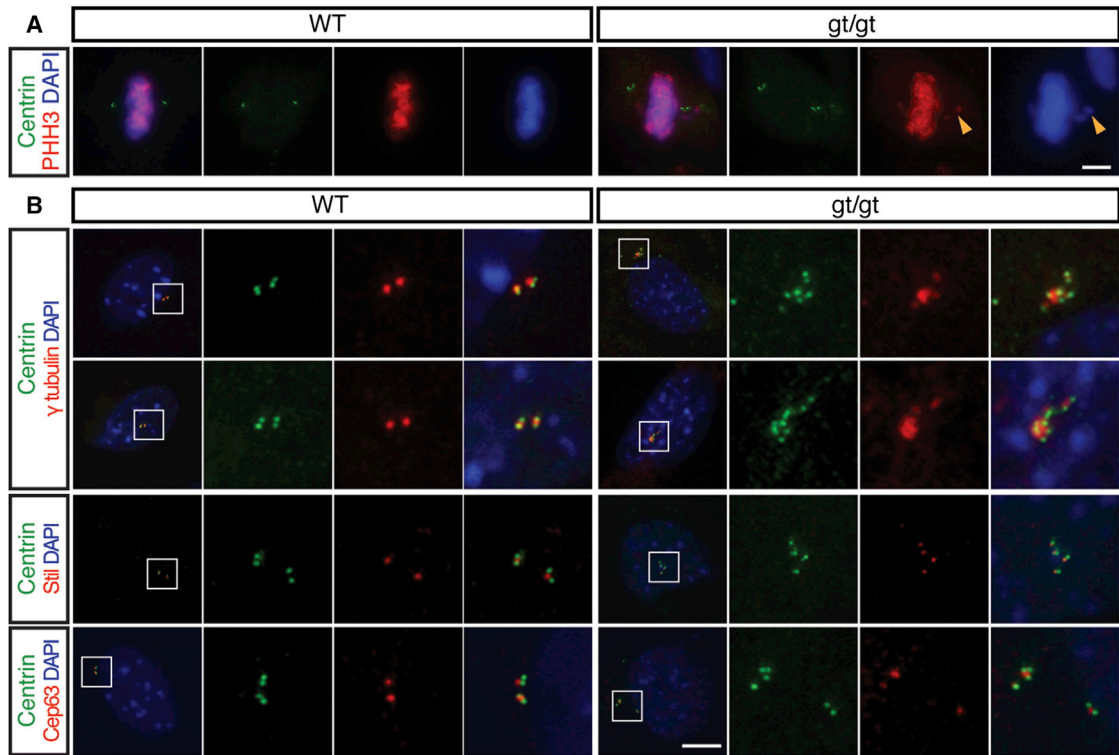
The identification of mutations in *KATNB1* suggests that mutations in *KATNA1*, encoding the catalytic katanin p60 subunit, might also cause microlissencephaly, given their strong biochemical and functional interactions. In our cohort of micro-

cephalic and lissencephalic pedigrees, we have not yet identified any individuals with *KATNA1* mutations. Complete loss of *KATNA1* function may be incompatible with embryonic survival, as is the case with *Drosophila* katanin p60 (Mao et al., 2014), or mutations in *KATNA1* may cause an entirely different human phenotype. Further characterization and sequencing in individuals will be necessary to more fully explore the human genetics of katanin mutations.

The essential roles of *KATNB1* in humans, mice, and zebrafish are somewhat surprising, given our knowledge of the role of the katanin complex from previous work, and illustrate the unique insight hypomorphic human mutations offers in uncovering novel regulators of early embryonic development. Katanin is a microtubule-severing enzyme necessary for meiotic spindle assembly (Mains et al., 1990; Srayko et al., 2006), determination of mitotic spindle length (Loughlin et al., 2011; McNally et al., 2006), severing at microtubule crossovers (Lindeboom et al., 2013; Zhang et al., 2013), axon outgrowth (Ahmad et al., 1999; Karabay et al., 2004; Yu et al., 2005), and cell motility (Zhang et al., 2011). Furthermore, katanin has been shown to be required for axonemal structure (Casanova et al., 2009; Dymek and Smith, 2012) and basal body release (Rasi et al., 2009). However, these functions all relate to katanin's microtubule-severing activity. Our data point to roles for the katanin complex that have not previously been described or even suspected based on its microtubule-severing function. The supernumerary cilia we observe are not remnants from previous cell cycles that have not been disassembled, but, rather, are formed de novo with each cell cycle. Furthermore, our data implicate katanin p80 in functions independent of targeting katanin p60 to the centrosome or regulating katanin p60 catalytic activity (Hartman et al., 1998; McNally et al., 2000).

Katanin p80, Centrioles, and Cilia

We present evidence showing katanin's involvement in control of centriolar number and centriolar type, as well as in ciliogenesis and Shh signaling, and in vivo evidence linking all three processes. *Katnb1*-deficient cells show a striking excess of centrioles, including multiple mother centrioles. In asymmetrical divisions of cortical progenitor cells, the mother centriole is preferentially inherited by the stem cell that continues dividing, whereas the daughter centriole is associated with the more differentiated cell. Moreover, the mother centriole is associated with a piece of ciliary membrane that serves to initiate a new cilium in the cell inheriting the more mature, mother centriole, allowing it to respond more quickly to extracellular growth signals, including Shh and IGF2 (Anderson and Stearns, 2009; Lehtinen et al., 2011; Paridaen et al., 2013; Piotrowska-Nitsche and Caspary, 2012; Saade et al., 2013). Although overduplication of centrioles has been produced by overexpression of genes such as *PLK4*, *SAS-6*, *STIL*, *CPAP*, and *CEP120* (Arquint and Nigg, 2014; Habedanck et al., 2005; Kleylein-Sohn et al., 2007; Lin et al., 2013; Peel et al., 2007; Strnad et al., 2007; Tang et al., 2011), or by loss of *CCDC14*, *CEP76*, *Lin-23*, and *Sel-10* (Firat-Karalar et al., 2014; Peel et al., 2012; Tsang et al., 2009), centriole overduplication does not always cause excess mother centrioles or cilia to form (Mahjoub and Stearns, 2012; Marthiens et al., 2013), as overexpression of *Plk4* in the mouse brain leads to

centrosomal overduplication and microcephaly, but without defects in cilia number or Shh signaling (Marthiens et al., 2013). Our findings of multiple mother centrioles in *Katnb1* mutant cells, and multiple cilia but with defective ciliary Shh signaling, suggest that katanin p80 may serve an essential role in the link between centriole and cilium to cell fate in the cortical ventricular zone.

The precise mechanism by which loss of katanin p80 causes centriole overduplication remains unexplored. Duplication of centrioles is normally limited to once per cell cycle, and presence of a daughter centriole inhibits centriole duplication (La Terra et al., 2005; Loncarek et al., 2008; Wong and Stearns, 2003). However, certain cell lines are capable of excess duplication when artificially arrested in S phase (Balczon et al., 1995), and overexpression of various centriolar and pericentriolar matrix proteins causes overduplication (Loncarek et al., 2008; Mahjoub, 2013).

Centriole duplication can occur from a template mother centriole or by de novo synthesis, which require similar factors (Khodjakov et al., 2002; La Terra et al., 2005). In the absence of katanin p80, both excessive templating of the mother centriole and unbridled de novo centriole synthesis are possibilities. Immunostaining and electron microscopy show centrioles clustered together, rather than scattered throughout the cell, suggesting that some templating may occur. However, the centrioles we observe are not paired in the classic orthogonal orientation of templated, duplicating centrioles and suggest the de novo pathway may nonetheless be active. Furthermore, centriole duplication has been proposed to be regulated by controlling the localization of duplication factors (Firat-Karalar et al., 2014). The increased microtubule stability with loss of katanin may prevent trafficking of positive and negative regulators of centriole duplication to and away from the centrosome, resulting in unbridled duplication.

There is emerging evidence in neurodevelopment for genes linking centrosome, spindle, and cilia biology. Ciliopathy syndromes are associated with rare brain malformations, though the mechanism by which they occur and their significance is still unclear (Lee and Gleeson, 2011; Nigg and Raff, 2009; Oh and Katsanis, 2012). Our results suggest that defects in cilia may cause isolated nervous system disease, potentially related to its roles in later development. Loss of two other centrosomal microcephaly genes, *CDK5RAP2* and *NDE1*, are known to cause excess centrosomes and multipolar spindles and have recently been shown to affect cilia length and number as well (Alkuraya et al., 2011; Bakircioğlu et al., 2011; Barrera et al., 2010; Bond et al., 2005; Kim et al., 2011; Lizarraga et al., 2010). Mutations in *NDE1* were the first identified cause of microlissencephaly

(Alkuraya et al., 2011; Bakircioğlu et al., 2011), with a phenotype very similar to that of *KATNB1* mutations, and katanin p80 physically interacts with Ndel1, a close paralog of Nde1 (Toyo-Oka et al., 2005). *Nde1* and *Cdk5Rap2* also encode centrosomal proteins essential for neurogenesis, though loss of neither *Nde1* nor *Cdk5Rap2* is as severe as *Katnb1* loss in mice (Barrera et al., 2010; Feng and Walsh, 2004; Lizarraga et al., 2010). An appealing model, therefore, is that *CDK5RAP2*, *NDE1*, and *KATNB1* may control the pathway limiting centriole duplication, and that the presence of excessive centrioles, particularly mother centrioles, in dividing neuroepithelial cells results in perturbed ciliary growth factor signaling, defective proliferation, and excessive cell death.

EXPERIMENTAL PROCEDURES

Human Subjects

A combination of homozygosity mapping, whole-exome sequencing, and targeted sequencing of coding exons within areas of homozygosity was performed and filtered as described in the Supplemental Experimental Procedures. All studies were reviewed and approved by the Institutional Review Board of Boston Children's Hospital, Harvard Medical School, and local institutions.

Animals

Targeted gene-trap ESCs (EUCOMM) were injected into C57BL/6 blastocysts to generate chimeric mice. Male chimeras were bred to WT C57BL/6 females (Charles River) to transmit the gene-trap allele. The mice were maintained on a C57/BL6 background. For pulse-labeling experiments, E12.5 timed pregnant mice were injected with 75 mg/kg BrdU intraperitoneally and euthanized 30 min later.

TALENs targeting the exon 6–intron 6 boundary of zebrafish *katnb1* (ENSDARG00000005456) were obtained from ZGENEBIO Biotech Co. Ltd (Table S2). To generate *katnb1* mutants, 150–200 pg of RNA was injected into one-cell-stage eggs (*albino/slc45a2*).
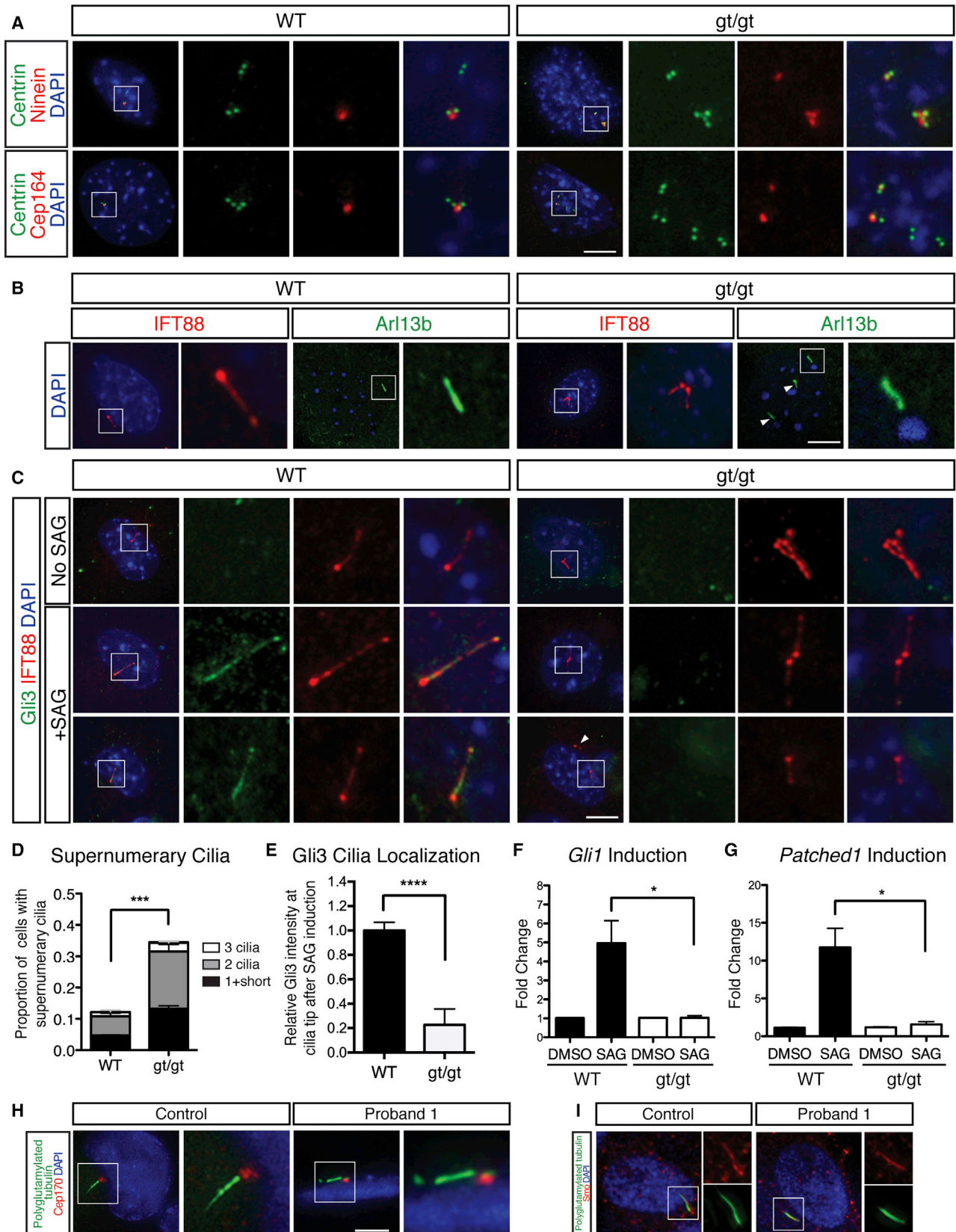
Culture Systems

Epstein-Barr virus-immortalized lymphoblastoid cell lines established from Proband 2 were maintained in RPMI-1640 (GIBCO) with 10% fetal bovine serum (FBS, GIBCO), and 1 mM penicillin and streptomycin (P/S). Primary fibroblasts were established from Proband 3 and were maintained in RPMI-1640 (GIBCO) with 10% FBS, and 1 mM P/S. Human iPSCs (Figure S2A) were generated using retroviral vectors encoding human *KLF4*, *SOX2*, *OCT4*, and *C-MYC* cDNA (Addgene) and grown in knockout DMEM with 20% knockout serum replacement, 2 mM L-glutamine, 1% NEAA, 0.1 mM β-mercaptoethanol, 0.1% P/S, and 4 ng/ml bFGF on irradiated fibroblast feeders. iPSCs were dissociated to form embryoid bodies (EBs) and induced in neural induction medium (DMEM/F12 supplemented with 20% KOSR, 2 mM L-glutamine, 0.2 mM NEAA, 0.1 mM 2-mercaptoethanol, and 1 mM sodium pyruvate) for 7 days. EBs were then adhered onto laminin-coated plates in neural precursor medium (neurobasal with 2 mM L-glutamine, 1% B27, 1% N2, and 20 ng/ml bFGF) for 7–14 days to form rosettes, which were manually isolated and expanded as NSCs in neural induction medium.

Figure 7. Loss of Katanin p80 Causes Centriole Overduplication

(A) Homozygous gt/gt MEFs have multipolar mitotic spindles and misaligned chromosomes (arrowhead). PHH3, phosphorylated histone H3. Scale bar, 10 um.

(B) Centrioles, labeled by Centrin, are overduplicated in homozygous gt/gt MEFs compared with wild-type MEFs. Centrosomal proteins γ-tubulin (top), Stil (middle), and Cep63 (bottom) associate with supernumerary centrioles with normal stoichiometry. Scale bar, 10 um.

(C) Serial transmission electron micrograph sections through centrosomes show multiple unpaired centrioles in gene-trap MEFs, whereas wild-type MEFs contain only one pair of centrioles. Arrowhead, centriole. Scale bar, 200 nm.

(D) Quantification of mitotic spindle abnormalities in (A). Unpaired t test, p < 0.0001.

(E) Quantification of centriolar overduplication in (B). Unpaired t test, p < 0.0001.

(F) Homozygous gt/gt MEFs grow more slowly than wild-type or gt/+ MEFs. Two-way ANOVA, p < 0.001.

See also Figure S6.

(legend on next page)

Trypsin-dissociated MEFs isolated from E13.5 mouse embryos were grown in DMEM, High Glucose (HyClone) with 15% FBS, and 1 mM P/S and L-glutamine. Cilia were induced by serum starvation for 48 hr in Optimem (GIBCO) media, then treated with DMSO or 100 nM SAG for an additional 24 hr.

Additional details are available in Supplemental Experimental Procedures.

Quantitative RT-PCR
See Supplemental Experimental Procedures.

Western Blotting
See Supplemental Experimental Procedures.

Immunostaining
See Supplemental Experimental Procedures.

SUPPLEMENTAL INFORMATION

Supplemental Information includes seven figures, two tables, one movie, and Supplemental Experimental Procedures and can be found with this article at http://dx.doi.org/10.1016/j.neuron.2014.12.017.

AUTHOR CONTRIBUTIONS

W.F.H. designed, performed, and analyzed experiments to characterize the mutations in Families 2 and 3; generated the gene-trap mouse line and zebrafish mutant lines; designed, performed, and analyzed all mouse and zebrafish experiments; helped analyze the centriolar and ciliary phenotypes; designed, performed, and analyzed EM experiments, and wrote the manuscript. O.P. designed, performed, and analyzed experiments relating to Family 1. T.B.-O. identified Family 3. A.K. and J.F.R. designed and performed immunostaining experiments in mouse cell lines, and identified and analyzed centriolar and ciliary phenotypes. K.H. generated the zebrafish mutant lines and designed, performed, and analyzed all zebrafish experiments. G.H.M. designed and performed initial genome-wide linkage studies, and G.H.M. and T.W.Y. designed and performed targeted capture sequencing on Family 3. M.B.W. performed and analyzed mouse BrdU labeling experiments and helped analyze centriole duplication phenotypes in Family 2 and mouse cell lines. C.B. analyzed the IBD mapping and exome sequencing of Family 1. G.S.R. and T.T.T. reprogrammed fibroblasts into iPSCs and performed immunostaining for Family 1. H.H. identified and A.M. and M.S. provided clinical information for Family 1. M.A.S. and J.N.P. organized clinical information and subject samples for Families 2 and 3. M.A-.D., A.A., M.A., and F.S.A. identified, provided clinical information for, and performed genetic analyses for Family 2. M.P.H. directed the zebrafish research. B.R. directed the research for Family 1. C.A.W. directed the overall research and wrote the manuscript.

ACKNOWLEDGMENTS

REFERENCES

Ahmad, F.J., Yu, W., McNally, F.J., and Baas, P.W. (1999). An essential role for katanin in severing microtubules in the neuron. J. Cell Biol. 145, 305–315.

Alkuraya, F.S., Cai, X., Emery, C., Mochida, G.H., Al-Dosari, M.S., Felie, J.M., Hill, R.S., Barry, B.J., Partlow, J.N., Gascon, G.G., et al. (2011). Human mutations in NDE1 cause extreme microcephaly with lissencephaly [corrected]. Am. J. Hum. Genet. 88, 536–547.

Anderson, C.T., and Stearns, T. (2009). Centriole age underlies asynchronous primary cilium growth in mammalian cells. Curr. Biol. 19, 1498–1502.

Arquint, C., and Nigg, E.A. (2014). STIL microcephaly mutations interfere with APC/C-mediated degradation and cause centriole amplification. Curr. Biol. 24, 351–360.

Ayoub, A.E., Oh, S., Xie, Y., Leng, J., Cotney, J., Dominguez, M.H., Noonan, J.P., and Rakic, P. (2011). Transcriptional programs in transient embryonic zones of the cerebral cortex defined by high-resolution mRNA sequencing. Proc. Natl. Acad. Sci. USA 108, 14950–14955.

Bakircioğlu, M., Carvalho, O.P., Khurshid, M., Cox, J.J., Tüysüz, B., Barak, T., Yilmaz, S., Caglayan, O., Dinçer, A., Nicholas, A.K., et al. (2011). The essential role of centrosomal NDE1 in human cerebral cortex neurogenesis. Am. J. Hum. Genet. 88, 523–535.

Balczon, R., Bao, L., Zimmer, W.E., Brown, K., Zinkowski, R.P., and Brinkley, B.R. (1995). Dissociation of centrosome replication events from cycles of DNA

Figure 8. In the Absence of Katanin p80, Fibroblasts Produce Supernumerary Cilia with Abrogated Shh Signaling

(A) Homozygous gt/gt MEFs contain multiple mother centrioles that label with Ninein (top) and Cep164 (bottom). Scale bar, 10 um.

(B) Homozygous gt/gt MEFs grow multiple cilia marked by IFT88 and Arl13b (right), while wild-type MEFs grow only a single cilium (left). Arrowheads, supernumerary cilia not shown in inset. Scale bar, 10 um.

(C) After stimulation by Smoothened agonist (SAG), gt/gt MEFs fail to relocate Gli3 to the cilium, indicating a deficit in Sonic hedgehog signaling (right). Wild-type MEFs robustly relocate Gli3 to the cilium after SAG stimulation (left). Scale bar, 10 um.

(E) Quantification of proportion of ciliated MEFs with supernumerary cilia from (B). Error bars represent mean ± SEM. Unpaired t test, p < 0.01.

(E) Quantification of cilial tip Gli3 intensity in SAG-stimulated cells from (C). Unpaired t test, p < 0.0001.

(F and G) Downstream Sonic hedgehog targets Gli1 (F) and Patched1 (G) are induced at lower levels following SAG stimulation in gt/gt MEFs compared with wild-type MEFs. Error bars represent mean ± SEM. Unpaired t test, p < 0.05.

(H) NSCs derived from Proband 1 do not grow supernumerary cilia. Scale bar, 10 um.

(I) After stimulation by Smoothened agonist (SAG), control and mutant NSCs show similar Smoothened (Smo) localization to the cilium. Scale bar, 10 um.

See also Figure S7.

synthesis and mitotic division in hydroxyurea-arrested Chinese hamster ovary cells. J. Cell Biol. *130*, 105–115.

Baron, M.H. (2013). Concise Review: early embryonic erythropoiesis: not so primitive after all. Stem Cells *31*, 849–856.

Barrera, J.A., Kao, L.-R., Hammer, R.E., Seemann, J., Fuchs, J.L., and Megraw, T.L. (2010). CDK5RAP2 regulates centriole engagement and cohesion in mice. Dev. Cell *18*, 913–926.

Belloni, E., Muenke, M., Roessler, E., Traverso, G., Siegel-Bartelt, J., Frumkin, A., Mitchell, H.F., Donis-Keller, H., Helms, C., Hing, A.V., et al. (1996). Identification of Sonic hedgehog as a candidate gene responsible for holoprosencephaly. Nat. Genet. *14*, 353–356.

Blanchette, M., Kent, W.J., Riemer, C., Elnitski, L., Smit, A.F.A., Roskin, K.M., Baertsch, R., Rosenbloom, K., Clawson, H., Green, E.D., et al. (2004). Aligning multiple genomic sequences with the threaded blockset aligner. Genome Res. *14*, 708–715.

Bond, J., Roberts, E., Springell, K., Lizarraga, S.B., Scott, S., Higgins, J., Hampshire, D.J., Morrison, E.E., Leal, G.F., Silva, E.O., et al. (2005). A centrosomal mechanism involving CDK5RAP2 and CENPJ controls brain size. Nat. Genet. *37*, 353–355.

Casanova, M., Crobu, L., Blaineau, C., Bourgeois, N., Bastien, P., and Pagès, M. (2009). Microtubule-severing proteins are involved in flagellar length control and mitosis in Trypanosomatids. Mol. Microbiol. *71*, 1353–1370.

Chiang, C., Litingtung, Y., Lee, E., Young, K.E., Corden, J.L., Westphal, H., and Beachy, P.A. (1996). Cyclopia and defective axial patterning in mice lacking Sonic hedgehog gene function. Nature *383*, 407–413.

Cooper, G.M., Stone, E.A., Asimenos, G., Green, E.D., Batzoglou, S., and Sidow, A.; NISC Comparative Sequencing Program (2005). Distribution and intensity of constraint in mammalian genomic sequence. Genome Res. *15*, 901–913.

Cridland, S.O., Keys, J.R., Papathanasiou, P., and Perkins, A.C. (2009). Indian hedgehog supports definitive erythropoiesis. Blood Cells Mol. Dis. *43*, 149–155.

Davydov, E.V., Goode, D.L., Sirota, M., Cooper, G.M., Sidow, A., and Batzoglou, S. (2010). Identifying a high fraction of the human genome to be under selective constraint using GERP++. PLoS Comput. Biol. *6*, e1001025.

Dubourg, C., Bendavid, C., Pasquier, L., Henry, C., Odent, S., and David, V. (2007). Holoprosencephaly. Orphanet J. Rare Dis. *2*, 8.

Dymek, E.E., and Smith, E.F. (2012). PF19 encodes the catalytic subunit of katanin, p60, and is required for assembly of the flagellar central apparatus in Chlamydomonas. J. Cell Sci. *125*, 3357–3366.

Feng, Y., and Walsh, C.A. (2004). Mitotic spindle regulation by Nde1 controls cerebral cortical size. Neuron *44*, 279–293.

Firat-Karalar, E.N., Rauniyar, N., Yates, J.R., 3rd, and Stearns, T. (2014). Proximity interactions among centrosome components identify regulators of centriole duplication. Curr. Biol. *24*, 664–670.

Greig, L.C., Woodworth, M.B., Galazo, M.J., Padmanabhan, H., and Macklis, J.D. (2013). Molecular logic of neocortical projection neuron specification, development and diversity. Nat. Rev. Neurosci. *14*, 755–769.

Habedanck, R., Stierhof, Y.-D., Wilkinson, C.J., and Nigg, E.A. (2005). The Polo kinase Plk4 functions in centriole duplication. Nat. Cell Biol. *7*, 1140–1146.

Hartman, J.J., Mahr, J., McNally, K., Okawa, K., Iwamatsu, A., Thomas, S., Cheesman, S., Heuser, J., Vale, R.D., and McNally, F.J. (1998). Katanin, a microtubule-severing protein, is a novel AAA ATPase that targets to the centrosome using a WD40-containing subunit. Cell *93*, 277–287.

Hayhurst, M., and McConnell, S.K. (2003). Mouse models of holoprosencephaly. Curr. Opin. Neurol. *16*, 135–141.

Higginbotham, H., Guo, J., Yokota, Y., Umberger, N.L., Su, C.-Y., Li, J., Verma, N., Hirt, J., Ghukasyan, V., Caspary, T., and Anton, E.S. (2013). Arl13b-regulated cilia activities are essential for polarized radial glial scaffold formation. Nat. Neurosci. *16*, 1000–1007.

Hildebrandt, F., Benzing, T., and Katsanis, N. (2011). Ciliopathies. N. Engl. J. Med. *364*, 1533–1543.

Hu, W.F., Chahrour, M.H., and Walsh, C.A. (2014). The diverse genetic landscape of neurodevelopmental disorders. Annu. Rev. Genomics Hum. Genet. *15*, 195–213.

Huangfu, D., and Anderson, K.V. (2005). Cilia and Hedgehog responsiveness in the mouse. Proc. Natl. Acad. Sci. USA *102*, 11325–11330.

Huangfu, D., Liu, A., Rakeman, A.S., Murcia, N.S., Niswander, L., and Anderson, K.V. (2003). Hedgehog signalling in the mouse requires intraflagellar transport proteins. Nature *426*, 83–87.

Karabay, A., Yu, W., Solowska, J.M., Baird, D.H., and Baas, P.W. (2004). Axonal growth is sensitive to the levels of katanin, a protein that severs microtubules. J. Neurosci. *24*, 5778–5788.

Karolchik, D., Barber, G.P., Casper, J., Clawson, H., Cline, M.S., Diekhans, M., Dreszer, T.R., Fujita, P.A., Guruvadoo, L., Haeussler, M., et al. (2014). The UCSC Genome Browser database: 2014 update. Nucleic Acids Res. *42* (Database issue), D764–D770.

Khodjakov, A., Rieder, C.L., Sluder, G., Cassels, G., Sibon, O., and Wang, C.-L. (2002). De novo formation of centrosomes in vertebrate cells arrested during S phase. J. Cell Biol. *158*, 1171–1181.

Kim, S., Zaghloul, N.A., Bubenshchikova, E., Oh, E.C., Rankin, S., Katsanis, N., Obara, T., and Tsiokas, L. (2011). Nde1-mediated inhibition of ciliogenesis affects cell cycle re-entry. Nat. Cell Biol. *13*, 351–360.

Kleylein-Sohn, J., Westendorf, J., Le Clech, M., Habedanck, R., Stierhof, Y.-D., and Nigg, E.A. (2007). Plk4-induced centriole biogenesis in human cells. Dev. Cell *13*, 190–202.

La Terra, S., English, C.N., Hergert, P., McEwen, B.F., Sluder, G., and Khodjakov, A. (2005). The de novo centriole assembly pathway in HeLa cells: cell cycle progression and centriole assembly/maturation. J. Cell Biol. *168*, 713–722.

Lee, J.E., and Gleeson, J.G. (2011). Cilia in the nervous system: linking cilia function and neurodevelopmental disorders. Curr. Opin. Neurol. *24*, 98–105.

Lehtinen, M.K., Zappaterra, M.W., Chen, X., Yang, Y.J., Hill, A.D., Lun, M., Maynard, T., Gonzalez, D., Kim, S., Ye, P., et al. (2011). The cerebrospinal fluid provides a proliferative niche for neural progenitor cells. Neuron *69*, 893–905.

Lin, Y.-N., Wu, C.-T., Lin, Y.-C., Hsu, W.-B., Tang, C.-J.C., Chang, C.-W., and Tang, T.K. (2013). CEP120 interacts with CPAP and positively regulates centriole elongation. J. Cell Biol. *202*, 211–219.

Lindeboom, J.J., Nakamura, M., Hibbel, A., Shundyak, K., Gutierrez, R., Ketelaar, T., Emons, A.M.C., Mulder, B.M., Kirik, V., and Ehrhardt, D.W. (2013). A mechanism for reorientation of cortical microtubule arrays driven by microtubule severing. Science *342*, 1245533.

Litingtung, Y., Dahn, R.D., Li, Y., Fallon, J.F., and Chiang, C. (2002). Shh and Gli3 are dispensable for limb skeleton formation but regulate digit number and identity. Nature *418*, 979–983.

Lizarraga, S.B., Margossian, S.P., Harris, M.H., Campagna, D.R., Han, A.-P., Blevins, S., Mudbhary, R., Barker, J.E., Walsh, C.A., and Fleming, M.D. (2010). Cdk5rap2 regulates centrosome function and chromosome segregation in neuronal progenitors. Development *137*, 1907–1917.

Loncarek, J., Hergert, P., Magidson, V., and Khodjakov, A. (2008). Control of daughter centriole formation by the pericentriolar material. Nat. Cell Biol. *10*, 322–328.

Loughlin, R., Wilbur, J.D., McNally, F.J., Nédélec, F.J., and Heald, R. (2011). Katanin contributes to interspecies spindle length scaling in Xenopus. Cell *147*, 1397–1407.

Lui, J.H., Hansen, D.V., and Kriegstein, A.R. (2011). Development and evolution of the human neocortex. Cell *146*, 18–36.

Mahjoub, M.R. (2013). The importance of a single primary cilium. Organogenesis *9*, 61–69.

Mahjoub, M.R., and Stearns, T. (2012). Supernumerary centrosomes nucleate extra cilia and compromise primary cilium signaling. Curr. Biol. *22*, 1628–1634.

Mahmood, S., Ahmad, W., and Hassan, M.J. (2011). Autosomal Recessive Primary Microcephaly (MCPH): clinical manifestations, genetic heterogeneity and mutation continuum. Orphanet J. Rare Dis. *6*, 39.

Mains, P.E., Kemphues, K.J., Sprunger, S.A., Sulston, I.A., and Wood, W.B. (1990). Mutations affecting the meiotic and mitotic divisions of the early Caenorhabditis elegans embryo. Genetics *126*, 593–605.

Mao, C.-X., Xiong, Y., Xiong, Z., Wang, Q., Zhang, Y.Q., and Jin, S. (2014). Microtubule-severing protein Katanin regulates neuromuscular junction development and dendritic elaboration in Drosophila. Development *141*, 1064–1074.

Marthiens, V., Rujano, M.A., Pennetier, C., Tessier, S., Paul-Gilloteaux, P., and Basto, R. (2013). Centrosome amplification causes microcephaly. Nat. Cell Biol. *15*, 731–740.

McNally, F.J., and Vale, R.D. (1993). Identification of katanin, an ATPase that severs and disassembles stable microtubules. Cell *75*, 419–429.

McNally, K.P., Bazirgan, O.A., and McNally, F.J. (2000). Two domains of p80 katanin regulate microtubule severing and spindle pole targeting by p60 katanin. J. Cell Sci. *113*, 1623–1633.

McNally, K., Audhya, A., Oegema, K., and McNally, F.J. (2006). Katanin controls mitotic and meiotic spindle length. J. Cell Biol. *175*, 881–891.

Mishra-Gorur, K., Çağlayan, A.O., Schaffer, A.E., Chabu, C., Henegariu, O., Vonhoff, F., Akgümüş, G.T., Nishimura, S., Han, W., Tu, S., et al. (2014). Mutations in KATNB1 cause complex cerebral malformations by disrupting asymmetrically dividing neural progenitors. Neuron *84*, this issue, 1226–1239.

Mount, S.M. (1982). A catalogue of splice junction sequences. Nucleic Acids Res. *10*, 459–472.

Neer, E.J., Schmidt, C.J., Nambudripad, R., and Smith, T.F. (1994). The ancient regulatory-protein family of WD-repeat proteins. Nature *371*, 297–300.

Nigg, E.A., and Raff, J.W. (2009). Centrioles, centrosomes, and cilia in health and disease. Cell *139*, 663–678.

Novarino, G., Akizu, N., and Gleeson, J.G. (2011). Modeling human disease in humans: the ciliopathies. Cell *147*, 70–79.

O'Donnell, L., Rhodes, D., Smith, S.J., Merriner, D.J., Clark, B.J., Borg, C., Whittle, B., O'Connor, A.E., Smith, L.B., McNally, F.J., et al. (2012). An essential role for katanin p80 and microtubule severing in male gamete production. PLoS Genet. *8*, e1002698.

Oh, E.C., and Katsanis, N. (2012). Cilia in vertebrate development and disease. Development *139*, 443–448.

Paridaen, J.T.M.L., Wilsch-Bräuninger, M., and Huttner, W.B. (2013). Asymmetric inheritance of centrosome-associated primary cilium membrane directs ciliogenesis after cell division. Cell *155*, 333–344.

Peel, N., Stevens, N.R., Basto, R., and Raff, J.W. (2007). Overexpressing centriole-replication proteins in vivo induces centriole overduplication and de novo formation. Curr. Biol. *17*, 834–843.

Peel, N., Dougherty, M., Goeres, J., Liu, Y., and O'Connell, K.F. (2012). The C. elegans F-box proteins LIN-23 and SEL-10 antagonize centrosome duplication by regulating ZYG-1 levels. J. Cell Sci. *125*, 3535–3544.

Piotrowska-Nitsche, K., and Caspary, T. (2012). Live imaging of individual cell divisions in mouse neuroepithelium shows asymmetry in cilium formation and Sonic hedgehog response. Cilia *1*, 6.

Rasi, M.Q., Parker, J.D.K., Feldman, J.L., Marshall, W.F., and Quarmby, L.M. (2009). Katanin knockdown supports a role for microtubule severing in release of basal bodies before mitosis in Chlamydomonas. Mol. Biol. Cell *20*, 379–388.

Roessler, E., Belloni, E., Gaudenz, K., Jay, P., Berta, P., Scherer, S.W., Tsui, L.C., and Muenke, M. (1996). Mutations in the human Sonic Hedgehog gene cause holoprosencephaly. Nat. Genet. *14*, 357–360.

Saade, M., Gutiérrez-Vallejo, I., Le Dréau, G., Rabadán, M.A., Miguez, D.G., Buceta, J., and Martí, E. (2013). Sonic hedgehog signaling switches the mode of division in the developing nervous system. Cell Rep. *4*, 492–503.

Senapathy, P., Shapiro, M.B., and Harris, N.L. (1990). Splice junctions, branch point sites, and exons: sequence statistics, identification, and applications to genome project. Methods Enzymol. *183*, 252–278.

Shi, Q., and King, R.W. (2005). Chromosome nondisjunction yields tetraploid rather than aneuploid cells in human cell lines. Nature *437*, 1038–1042.

Srayko, M., O'toole, E.T., Hyman, A.A., and Müller-Reichert, T. (2006). Katanin disrupts the microtubule lattice and increases polymer number in *C. elegans* meiosis. Curr. Biol. *16*, 1944–1949.

Strnad, P., Leidel, S., Vinogradova, T., Euteneuer, U., Khodjakov, A., and Gönczy, P. (2007). Regulated HsSAS-6 levels ensure formation of a single procentriole per centriole during the centrosome duplication cycle. Dev. Cell *13*, 203–213.

Tang, C.-J.C., Lin, S.-Y., Hsu, W.-B., Lin, Y.-N., Wu, C.-T., Lin, Y.-C., Chang, C.-W., Wu, K.-S., and Tang, T.K. (2011). The human microcephaly protein STIL interacts with CPAP and is required for procentriole formation. EMBO J. *30*, 4790–4804.

Thornton, G.K., and Woods, C.G. (2009). Primary microcephaly: do all roads lead to Rome? Trends Genet. *25*, 501–510.

Tong, C.K., Han, Y.-G., Shah, J.K., Obernier, K., Guinto, C.D., and Alvarez-Buylla, A. (2014). Primary cilia are required in a unique subpopulation of neural progenitors. Proc. Natl. Acad. Sci. USA *111*, 12438–12443.

Toyo-Oka, K., Sasaki, S., Yano, Y., Mori, D., Kobayashi, T., Toyoshima, Y.Y., Tokuoka, S.M., Ishii, S., Shimizu, T., Muramatsu, M., et al. (2005). Recruitment of katanin p60 by phosphorylated NDEL1, an LIS1 interacting protein, is essential for mitotic cell division and neuronal migration. Hum. Mol. Genet. *14*, 3113–3128.

Tsang, W.Y., Spektor, A., Vijayakumar, S., Bista, B.R., Li, J., Sanchez, I., Duensing, S., and Dynlacht, B.D. (2009). Cep76, a centrosomal protein that specifically restrains centriole reduplication. Dev. Cell *16*, 649–660.

Wang, X., Tsai, J.-W., Imai, J.H., Lian, W.-N., Vallee, R.B., and Shi, S.-H. (2009). Asymmetric centrosome inheritance maintains neural progenitors in the neocortex. Nature *461*, 947–955.

Willaredt, M.A., Hasenpusch-Theil, K., Gardner, H.A.R., Kitanovic, I., Hirschfeld-Warneken, V.C., Gojak, C.P., Gorgas, K., Bradford, C.L., Spatz, J., Wölfl, S., et al. (2008). A crucial role for primary cilia in cortical morphogenesis. J. Neurosci. *28*, 12887–12900.

Wong, C., and Stearns, T. (2003). Centrosome number is controlled by a centrosome-intrinsic block to reduplication. Nat. Cell Biol. *5*, 539–544.

Yu, W., Solowska, J.M., Qiang, L., Karabay, A., Baird, D., and Baas, P.W. (2005). Regulation of microtubule severing by katanin subunits during neuronal development. J. Neurosci. *25*, 5573–5583.

Zhang, Z., Li, J., Zhao, X.-Q., Wang, J., Wong, G.K.-S., and Yu, J. (2006). KaKs_Calculator: calculating Ka and Ks through model selection and model averaging. Genomics Proteomics Bioinformatics *4*, 259–263.

Zhang, D., Grode, K.D., Stewman, S.F., Diaz-Valencia, J.D., Liebling, E., Rath, U., Riera, T., Currie, J.D., Buster, D.W., Asenjo, A.B., et al. (2011). Drosophila katanin is a microtubule depolymerase that regulates cortical-microtubule plus-end interactions and cell migration. Nat. Cell Biol. *13*, 361–370.

Zhang, Q., Fishel, E., Bertroche, T., and Dixit, R. (2013). Microtubule severing at crossover sites by katanin generates ordered cortical microtubule arrays in Arabidopsis. Curr. Biol. *23*, 2191–2195.